2-D Ising Model Simulation: Investigation of Square and Triangular Lattices

Aaron Miller
17322856
milleraa@tcd.ie
JS computational methods project

Lecturer: Stephen Power
Trinity College Dublin

(Dated: December 28, 2019)

CONTENTS

I. ABSTRACT

In this report, I investigate the two dimensional Ising model through Python 3.7. I explored the model configured as a square lattice, with no external magnetic field, and the dimensionless magnetic interaction strength $J = 1$. I then investigated the effects of applying a magnetic field, and changing the geometry to that of a triangular lattice. I observed phase transitions for both lattice types after their critical temperature points. The square transitions from ferromagnetic, to a paramagnetic disordered phase [FIG 6], while the triangular lattice undergoes a shift from the ferromagnetic phase to a ferrimagnetic phase [FIG. 9], as the temperature increases. I observed a state of the system before the critical point where neither spin dominated, and the system was in an equilibrium. I estimated the critical temperature for the square, and triangular lattices to be $k_b T_c^{\square} = 2.3J$, and $k_b T_c^{\triangle} = 3.9J$. The first value is close to the theoretical value of $k_b T_c^{\square} = 2.269J$ [3]. There is no analytic solution, or analytic critical temperature for the triangular lattice. The application of magnetic field has the effect of polarising the spins in the direction of the field. I also found that the triangular lattice was able to resist this polarisation of the applied field better then the square lattice below the critical temperature, due to the increased number of connections each point has. When I flipped the sign of the magnetic interaction the expected ferrimagnetic aligning was observed in both lattices. I include various *gif* files showing the evolution of the system for different configurations.

II. INTRODUCTION

A. Magnetism

Magnetism is a class of phenomena which occur due to magnetic fields, magnetic moments of particles, and the motion of electric currents. There are three main types of magnetism. Ferromagnetism is the way in which materials, for example iron, form permanent magnets [FIG. 1 (a)]. This is a purely quantum mechanical effect, due to the magnetic spins of the electrons all aligning in a certain direction and, to the Pauli exclusion principle [1]. Ferromagnets stay magnetised after exposure to external magnetic fields, due to the field aligning the magnetic spins in a unified direction. In this project we will be simulating a ferromagnetic system, using the Ising model. Ferrimagnetism is where the moments are ordered in areas of opposing, and agreeing spin. [FIG. 1 (b)]. Antiferromagnetism is when the moments are arranged in a reoccurring pattern [FIG. 1 (c)].

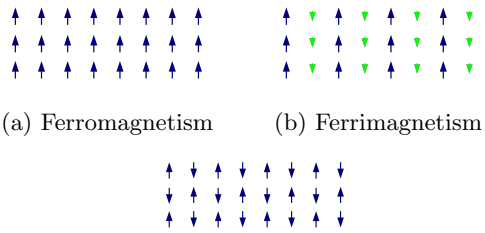

(a) Ferromagnetism (b) Ferrimagnetism

(c) Antiferromagnetism

FIG. 1: Ordering of magnetic moments for different types of magnetism

a. Curie Temperature

This is the temperature above which ferromagnetic materials lose their magnetism, due to thermal noise disrupting any alignment that the atoms my have had below that point. In iron, the Curie point is about 770°[2].

B. Ising Model

The Ising model is a simplified model of a magnet. For our 2-Dimensional model in question, we consider a fixed lattice or grid of points. For each of these points k, we attribute a 'spin'. In normal non-magnetic materials, this model would not apply as these magnetic spins are randomly aligned. However in magnetic materials like iron where the spins align, it is valid. The spin, σ_k, takes values of either 1 or -1. We define the non dimensional hamiltonian H, of the system to be,

$$\beta H'(\sigma) \equiv H(\sigma) = -J \sum_{\langle (i,j),(k,l)\rangle} \sigma_{(i,j)}\sigma_{(k,l)} - B\sum_{(i,j)} \sigma_{(i,j)}. \tag{1}$$

Where B is the nondimensionalized external magnetic field, $\beta = (Tk_b)^{-1}$ (units of $1/Joules$), and J is a parameter of the particle interaction. In the presence of no external B field,

$$H(\sigma) = -J \sum_{\langle (i,j),(k,l)\rangle} \sigma_{(i,j)}\sigma_{(k,l)}, \tag{2}$$

where we have assumed each of the neighbouring points σ_i and σ_j have the same strength of magnetic interaction J. This is the mean field approximation. We also assume that only the spins of the nearest neighbours interact, the sum over $\langle (i,j),(k,l)\rangle$ means just this. FIG. 2 illustrates the model. For the square lattices the curie point is $k_b T_c^{\square} = 2.269J$, derived by Onsagner in 1944. [3]

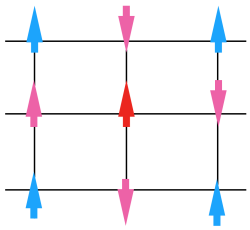

FIG. 2: Ising model lattice. Only the red, and pink spins interact as shown.

C. Calculating Observables

From methods in statistical physics, we can calculate observables of the system. I will omit the proofs of the following thermodynamic formulas as it is beyond the scope of my investigation, however it is discussed at length by *Richard Fitzpatrick* in his online notes [6]. The average energy per spin is

$$\langle E\rangle = \left\langle \sum_{\langle i,j\rangle} H_{ij} \right\rangle = \frac{1}{2}\left\langle \sum_{(i,j)} H_{ij} \right\rangle, \tag{3}$$

where $H_{i,j}$ is the energy of the site (i,j).The average magnetisation per spin,

$$\langle M\rangle = \frac{1}{N^2}\sum_{(i,j)} \sigma_{(i,j)}. \tag{4}$$

The sum over (i,j) is taken over the entire lattice. We expect that the average magnetism below the curie point in the absence of an external field should be either -1 or 1 forsquare and triangular lattices, and after it

should approach 0 as the thermal noise interferes and the system becomes disordered.

For the specific heat capacity,

$$C_V = \frac{1}{k_b T^2}\left(\langle E^2\rangle - \langle E\rangle^2\right) = \frac{s_E^2}{k_b T^2}, \tag{5}$$

and and the magnetic susceptibility,

$$\chi = \frac{1}{k_b T}\left(\langle M^2\rangle - \langle M\rangle^2\right) = \frac{s_M^2}{k_b T}, \tag{6}$$

where s_M^2 and s_E^2 are the standard deviations of M and E respectively. From our thermodynamic knowledge, these variables are derivatives of the Gibbs free energy and should be discontinuous when plotted as a function of temperature, at the point of phase transition.

D. Advanced Investigation: Triangular lattice, and External magnetic field

a. *Triangular lattice*

The main difference with this lattice is that each site now has 6 nearest neighbours. FIG. 3 below illustrates this. The physics described by the hamiltonian in Eq. 1 still applies but now we must account for extra neighbours. The critical point, and exact solutions to the specific heat, magnetisation, and susceptibility is unknown.

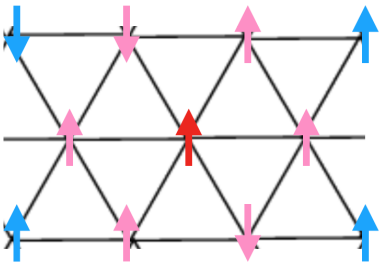

FIG. 3: Ising model triangular lattice. Only the red, and pink spins interact as shown.

b. *Application of external magnetic field B*

When we apply an external magnetic field to the system, the hamiltonian is of the form described by Eq. 1. The system should now exhibit a bias to arrange in the direction of the B field.

III. METHODOLOGY

A. Metropolis Algorithim

a. *Marcov chains*

A Marcov chain is a system describing a sequence of events, where the next event is only dependant on the current state. In our case, the event is the spin flip. This is probabilistically determined by the spin of the nearest neighbours which define the current state (see FIG. 2/3).

b. *The algorithm*

This algorithm is the principal method we use to solve this problem of the Ising model. The algorithm is based on Marcov chains. As we repeatedly update the system, it implements the Ising model.

- We start with a random configuration of spins, $s_0 = \{\sigma_{0,0}, \sigma_{0,1}, ...\sigma_{0,n^2}\}$, for $\sigma_{0,i} = \pm 1$ and $i \in \{1, 2..n\}$ (Note: the subindices denote iteration and position respectively), for our $n \times n$ lattice. This step initialises the Markov chains.
- We now need to update s_0 to s_1 by updating all of $\sigma_{0,i}$ depending only on its neighbours. This is realised by:
  - i) Calculating the change in energy ΔH_i from Eq.1.
    - When we flip the spin at the site ($\sigma_{(i,j)} \to -\sigma_{(i,j)}$), we can trivially show from Eq.1 that
    $$\Delta H \equiv \Delta E = 2J\sigma_{(i,j)} \sum_{\langle k,l\rangle} \sigma_{(k,l)} \tag{7}$$
  - ii) Then we accept of reject the flip by the criterion:
    - If $\Delta H_i \geq 0$ accept the flip (ie. $\sigma_{0,0} \to \sigma_{1,0} = -\sigma_{0,0}$) with probability $e^{-\Delta H_i \beta}$
    - Else, if $\Delta H_i \leq 0$ accept the transition.

The second step is then repeated for many iterations until the characteristics of the model are developed clearly.

B. Implementation to code

1. *Square Lattice*

a. *Initialising a grid of random spins*

I used the numpy *random.choice* to create a random $N \times N$ grid of spins $(-1, 1)$. Initially I was using a *for* loop to loop over a grid of points and change grid point to ± 1. However, the numpy function initialised it more efficiently.

b. Plotting and animating

To plot the lattice, I used *matshow* from the matplotlib library. This function attributed a colour for each ± 1 and plotted the state. This was an excellent indicator to test my code later on in the project. In order to animate the states, I used a combination of *matshow* and *Funcanimation*. I found difficulty in saving the animations when using the *%matplotlib* command to turn my notebook into a matplotlib notebook to view the animation. This was resolved by remaining in a python notebook, and using the *imagewick* writer to save it. To plot the triangular lattice I used a scatterplot and offset the points to form a triangular lattice. The colour argument of scatterplot was tricky, as it did not accept 2D arguments, so I flattened the array and passed it.

c. Implementing the fitness function

Implementing the model follows closely from the discussion of the algorithm in III. A. b). I started off by initialising a function which updated the 'fitness', or energy of a point according to its neighbours and Eq. 7. I initialised another grid to keep track of the fitness of each point on the grid. In order to deal with the fact we are dealing with a finite sized grid, I had to force periodicity on the crystal by imposing Born-von Karman Boundary Condition [5]. This means that when we reach one end of the lattice, the next neighbour is the first site on the other side (ie: the next x neighbour of $\sigma_{(N-1,j)}$ is $\sigma_{(0,j)}$). This was realised by use of the modulo operator when applied to the indices of the grid coordinates in fitness function.

d. Implementing the acceptance function

The acceptance function determines if the spin flips of not. This was implemented according to III. A. b), using if statements. For the square lattice, there were only a couple of discrete values of energy. That is, $\Delta E = [-8J, -4J, 0, 4J, 8J]$. As I needed to calculate for the cases where $\Delta E > 0$, I only needed to calculate two probabilities for the case of $\Delta E = [4J, 8J]$. This was calculated outside the function to stop unnecessary repeated calculations.

e. Simulating the system

Finally, I wrote the function which simulates the system. It consists of a while loop with a nested for loop. The loop ends when it iterates until a stopping iteration, while the inner loop sweeps over all the indices of the grid. At each of the grid coordinates, the acceptance function was called and the spin was updated accordingly. I updated and stored the values of the fitness of the point and its neighbours during the inner loop. I then recorded thermodynamic averages of the system after each full sweep. Heat capacity and magnetic susceptibility were calculated by employing the *numpy* functions std, and mean. This part of the code caused me the most pain. Originally I was thought I had to update the lattice by selecting a random point and then updating that point accordingly. This method somewhat worked, however convergence to the expected values of the system was much slower.

2. Triangular Lattice

The triangular lattice closely resembles the square lattice. All the neighbours are equidistant from the central point, which is the same case as the square lattice. Thus due to the relationship between distance between points, and the magnetic dipole moment, we can say that the lattice shown in FIG. 4 below is equivalent to the square lattice with extra points.

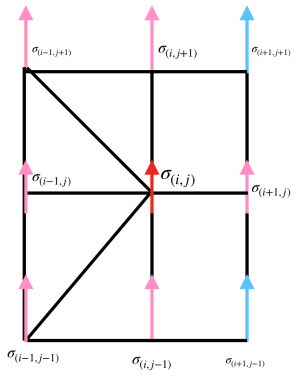

FIG. 4: Triangular lattice, red, and pink spins interact.

Now it is clear we only need to go back and account for the two extra terms $\sigma_{(i-1,j\pm1)}$ in order to implement this correctly. This was done so in the triangular lattice.

3. Accounting for external magnetic field

The magnetic field was easily implemented into the existing code. It was accounted for in the fitness function where I added the extra B term from Eq. 1.

IV. RESULTS AND DISCUSSION

A. Analysis of the Square Lattice

FIG. 5 illustrates the absolute value of total magnetism of the system, M, against the 'state' ie: the number updates the system has run through. It displays the average rate of convergence to a state of thermo-

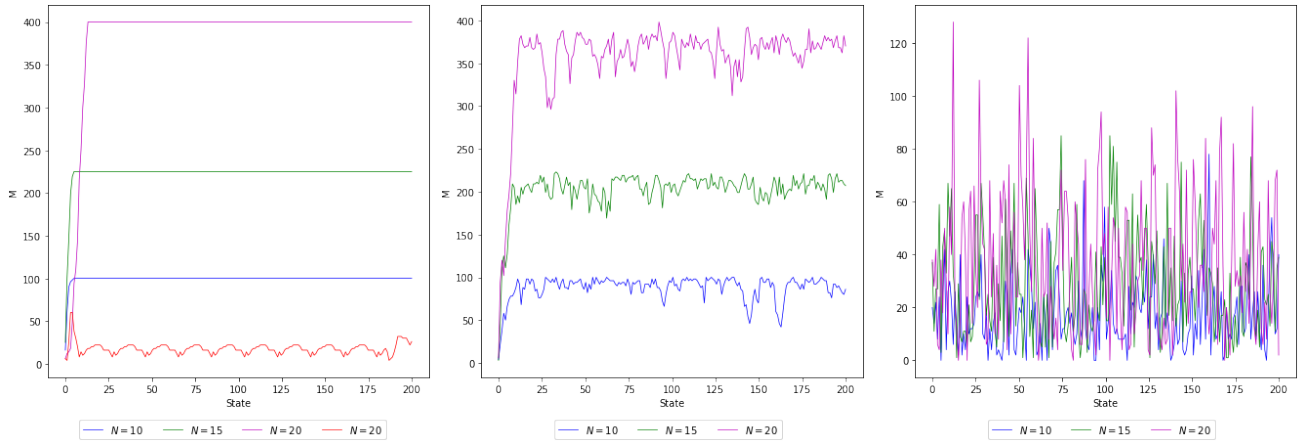

(a) $k_bT = 0.5J$ (b) $k_bT = 2J$ (c) $k_bT = 3.5J$

FIG. 5: Convergence of states a variety of temperatures, and gridsizes, $J = 1$

dynamic equilibrium for our model. We see that for lower temperatures below the predicted Curie point of $k_bT = 2.269J$ [FIG. 5 (a)], the system converges to a constant total magnetism equal to the number of grid points squared, N^2. This corresponds to the grid being in a total ± 1 spin state. It takes about 25 updates of the system to reach this predicted state usually. However the red line corresponding to a 20×20 grid, counters this idea. It doesn't seem to converge within the usual number of states, rather the system seems to be caught in a periodic equilibrium where neither spin is dominating. This corresponds to two large travelling domains of opposite spins. These domains persist at lower temperatures, however at higher temperatures below the critical point the equilibrium breaks due to thermal noise. Due to this, I used 200 warm up, and 100 counted runs to take averages over. FIG. 13 in the appendix illustrates the varying rate of convergence with temperature.

As the temperature nears the Curie point [FIG. 5 (b)], the graph no longer makes a clean straight line. This is due to the heat increasing the probability of a random spin flip. We see at high temperatures, [FIG. 5 (c)], the magnetism is unpredictable, and no spin dominates. The grid size N is related to the number of updates until convergence. Due to this and to lower computation time, the majority of data obtained will be from a 7×7 lattice.

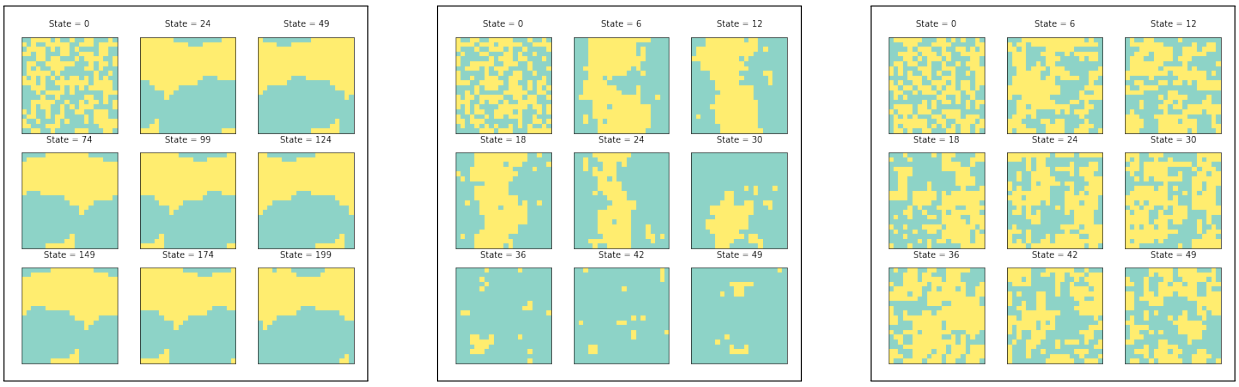

(a) $k_bT = 0.5$ (b) $k_bT = 2$ (c) $k_bT = 3.5$

FIG. 6: Convergence over 50 states, on a 20×20 lattice.

FIG. 6 shows the convergence of a 20×20 lattice. In all cases, pockets of ± 1 spin have formed, and as expected the system exhibits ferromagnetism. Now, (a) displays the states of the aforementioned red line from FIG. 5 (a). It shows that no one spin entirely dominates and there are large non-static domains of the same spin. This corresponds to the total magnetism floating around $|M| = 0$. For the higher temperature, (b) these large pockets are broken up due to increased thermal noise, so there are less instances of the spin domains occurring. There are random small pockets of opposing spin in the higher states due to noise. These correspond to the fluctuations observed in FIG. 5 (b). For (c) no spin dominates, however we see ferromagnetic aligning in small domains. To see this in action, view the animated $gifs$ attached to this document.

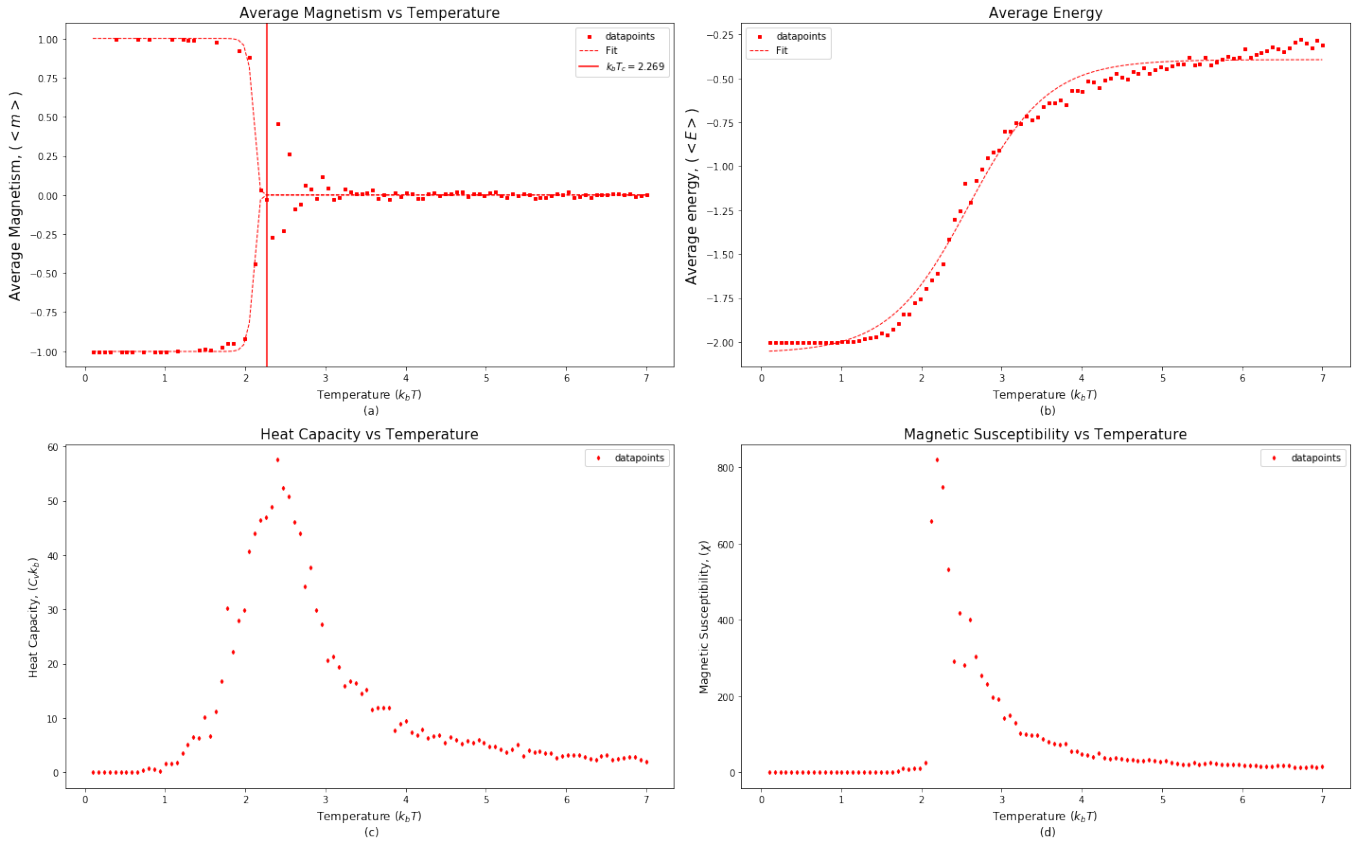

FIG. 7: Dimensionless thermodynamic quantities, for a 7×7 square lattice, $J = 1$.

FIG. 7 plots the average magnetism (a), average energy (b), heat capacity (c), and magnetic susceptibility (d) all against temperature for a 7×7 lattice. Note all these values are dimensionless.

FIG. 7 (a) shows bifurcation at $Tk_b \approx 2.3J$, which is our Curie point and it agrees well with theory. The bifurcation is due to there being no preference to ± 1 alignment below the curie point. It also shows the convergence to 0 as the temperature crosses the Curie point. This is an indication of a phase transition occurring. The curve has been fitted with a stretched exponential fit for comparison purposes. From this fit we see that our observed value for T_c, is close to our theoretically predicted value. The discrepancy is most likely due to our approximation of periodic boundary conditions for our lattice and because lattices taking longer to converge near T_c .

From (b) we see due to the amount of neighbours (4) and all the spins being aligned near $T \approx 0$, the average energy is $-2J = -2$. As the temperature increases the average energy increases, and tends towards 0 corresponding to a system of opposing spin. I used a *tanh* fit for this curve.

FIG. 7. (c) and (d) illustrate large spikes in the heat capacity, and magnetic susceptibility respectively near the theoretical $T_c^{\square}$. This is an example of discontinuous derivatives of the Gibbs free energy, and the average energy being a continuous function of temperature, are indications that a phase transition has occurred.

B. Triangular lattice

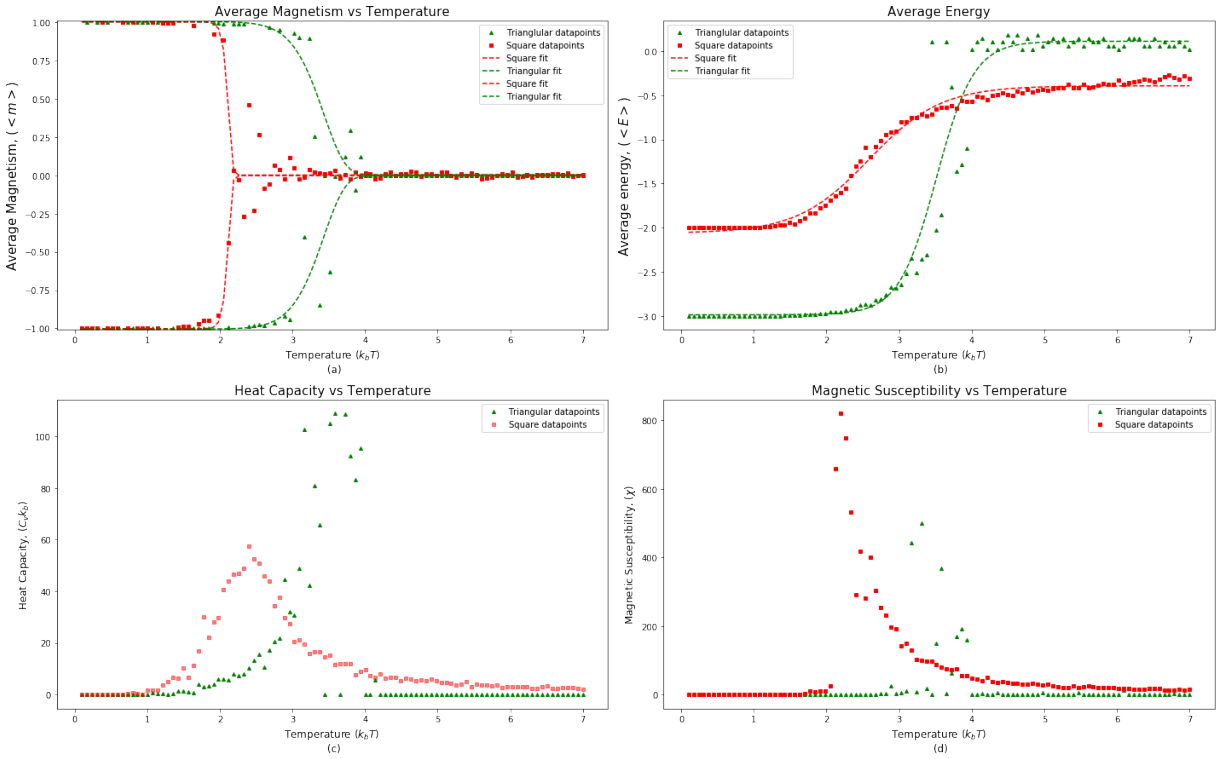

FIG. 8: Quantities compared, for 7×7 square, and triangular lattices $J = 1$.

FIG. 8 shows the difference between our results for the triangular and square lattices. From (a), I estimate $T_c^{\triangle} \approx 3.9$. The triangular lattice exhibits graphically similar properties to the square lattice in (a) and (b), but with a positive shift in the critical temperature. From (b) we observe as expected the $< E > \rightarrow -3J$ as $T \rightarrow 0$.

The peak of the heat capacity of the triangular lattice is greater then the square lattice. The heat capacity also tends to zero immediately after the peak. This is due to the increased number of connections in the triangular lattice, speeding up the number updates needed for convergence. The magnetic susceptibility exhibits this property however the peak of is smaller then the squares.

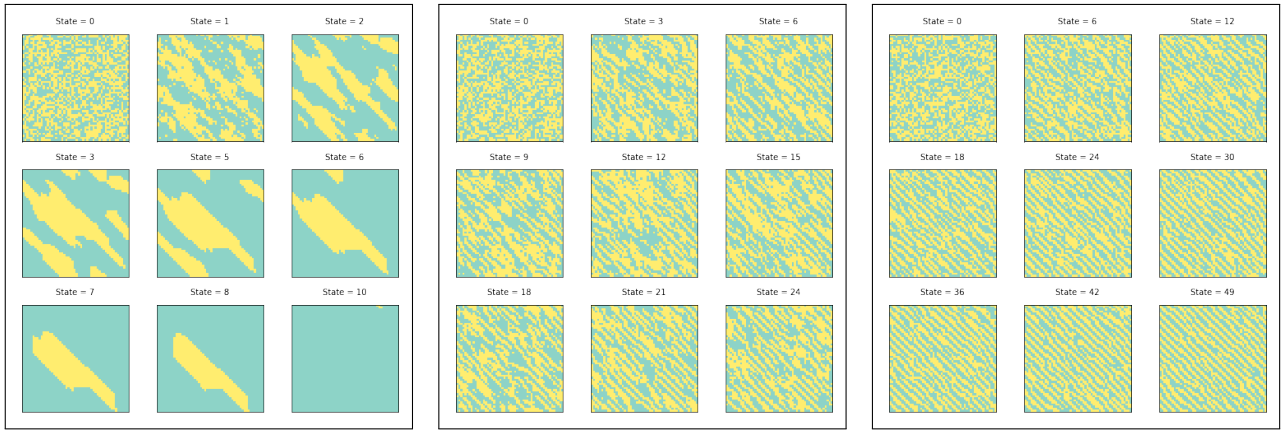

(a) $k_bT = 0.5$ (b) $k_bT = 4.0$ (c) $k_bT = 10.0$

FIG. 9: 52×52 triangular lattice, over a variety of states.

FIG. 9 displays the evolution of the system over a number of states. It shows in all cases domains of diagonal, linear spins. In (a) at a low temperature, the lattice converges as expected to a uniform spin. Past and at the Curie point the domains resemble ferrimagnetism, however before the Curie point ferromagnetism occurs.

C. External magnetic field

Now, we investigate the application of an external magnetic field B to our model. Below I have graphed the average magnetism and energy for an applied magnetic field in the range $-2 \leq B \leq 2$, for 3 temperatures and both lattices. I have chosen the temperatures so that they show the response of the lattice before, around, and after their respective critical temperatures. I have acquired data for 2 units above and 1.5 units below the critical temperature.

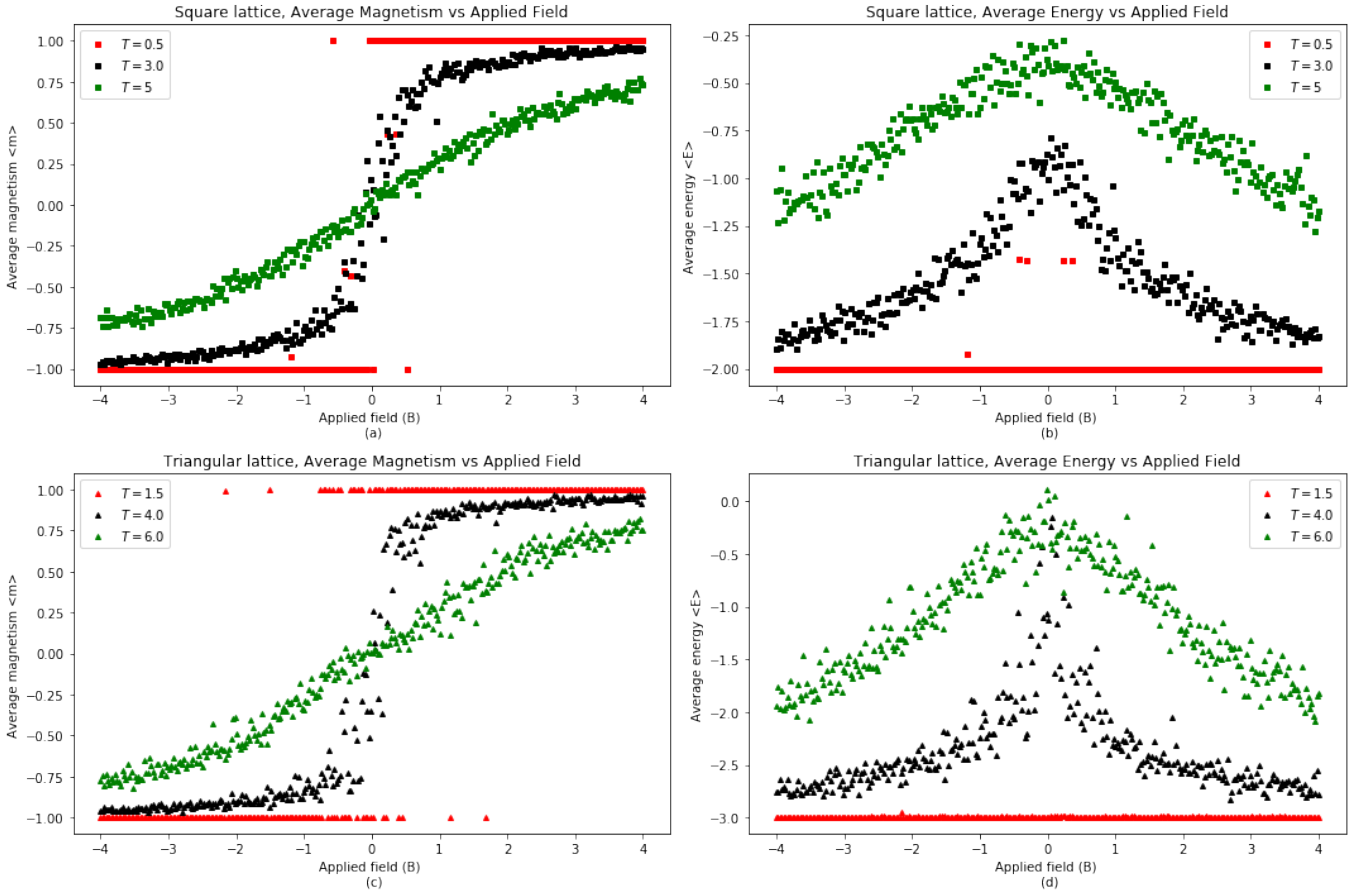

FIG. 10: Quantities compared at three different temperatures for the 7×7 square [(a), (b)], and triangular [(c), (d)] lattice with $J = 1$.

FIG. 10 shows that the lattices respond very similarly to this temperature range. Below the critical temperature, the average magnetism [(a), (c)] is a discontinuous step function of the applied field in both cases. The triangular lattice is able to resist the bias of the field better then the square lattice below the critical temperature, as the area of overlap where the system can be entirely spin ± 1, about $B = 0$ is $\Delta B = \pm 0.5$ [(c)]. At the critical temperature, the functions transition at the step has become smoother.After the point, it is essentially smooth. This is due to the the magnetic field forcing the system into alignment. A notable difference between the lattices is, at the lower temperature, as the field approaches 0 in (c) there is a greater affinity of the systems total spin to oppose that of the field.

In terms of the energy, we see what we expect. In both cases, and at all temperatures, the asymptotes tends towards energy values of -2 (b), and -3 (d). These correspond to the entire lattice being in ± 1 spin state as previously mentioned. For the lower temperatures, the magnetism is uniformly aligned across this field range. When the temperature increases, this uniformity is broken due to increased thermal noise.

D. Flipping of magnetic interaction J

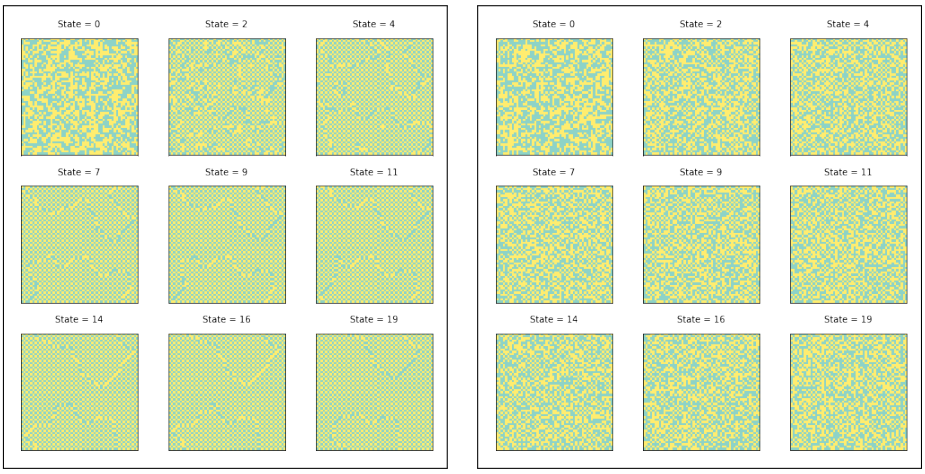

(a) $k_bT = 0.5$ (b) $k_bT = 5.0$

FIG. 11: 52×52 square lattice over a few states, $J = -1$.

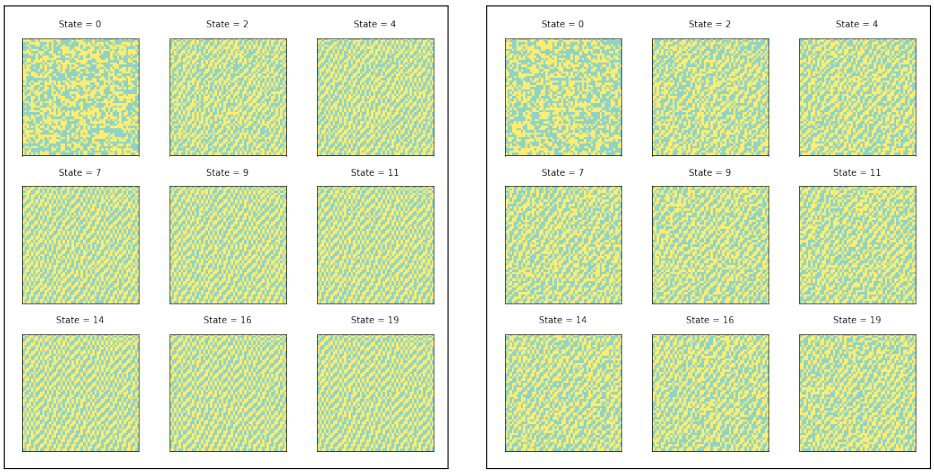

(a) $k_bT = 0.5$ (b) $k_bT = 5.0$

FIG. 12: 52×52 triangular lattice over a few states, $J = -1$.

Here we see the effects of inverting the sign of magnetic spin interaction, J. FIG. 11/12 shows the square/triangular lattices. For 11 (a), we see the predicted antiferromagnetic aligning of the spins. There are lines of defects present in the later states here. 12 (1) shows similar ferromagnetic aligning as the system progresses. At higher temperatures in 11/12 (b), we see disorder, and only minor ferromagnetic characteristics due to larger domains being disrupted by thermal effects.

V. CONCLUSION

From investigating the Ising model, I am amazed that such rich physics emerges from such a simple construction. I believe that I have successfully implemented the model with an external magnetic field for the triangular and square lattices. I initially investigated the model for $J = 1$. There was a definite phase transition in both lattices evident here, between the ferromagnetic and the disordered, paramagnetic phase of the square lattice [FIG 6]. For

the triangular lattice, I observed a shift from the ferromagnetic phase to a ferrimagnetic phase [FIG. 9].

I found that the model took on average, a total number of 25 updates to 'warm up' [FIG. 5], and reveal features of its underlying statistical processes. This was dependant however on the system size and given more time, I would have investigated this relationship. For the square 7×7 lattice, I estimate $k_b T_c^{\square} = 2.3J$. This value is close to the theoretical value of $k_b T_c^{\square} = 2.269J$. A reason for the discrepancy may have been the use of a small lattice, where an assumption in deriving the critical temperature, is an infinitely large one. If I had the time and computation power, I would have investigated this hypothesis.

For the triangular 7×7 lattice, I estimated $k_b T_c^{\triangle} = 3.9J$. I found the application of the the magnetic field had the effect of polarising the spins in the direction of the field. I also found that the triangular lattice is able to resist the bias of the applied field better then the square lattice below the critical temperature. When I flipped the sign of the magnetic interaction, the expected ferrimagnetic aligning was observed in the square lattice and also the triangular. I attach animated *gif* files of the different system configurations evolving with this document.

VI. APPENDIX

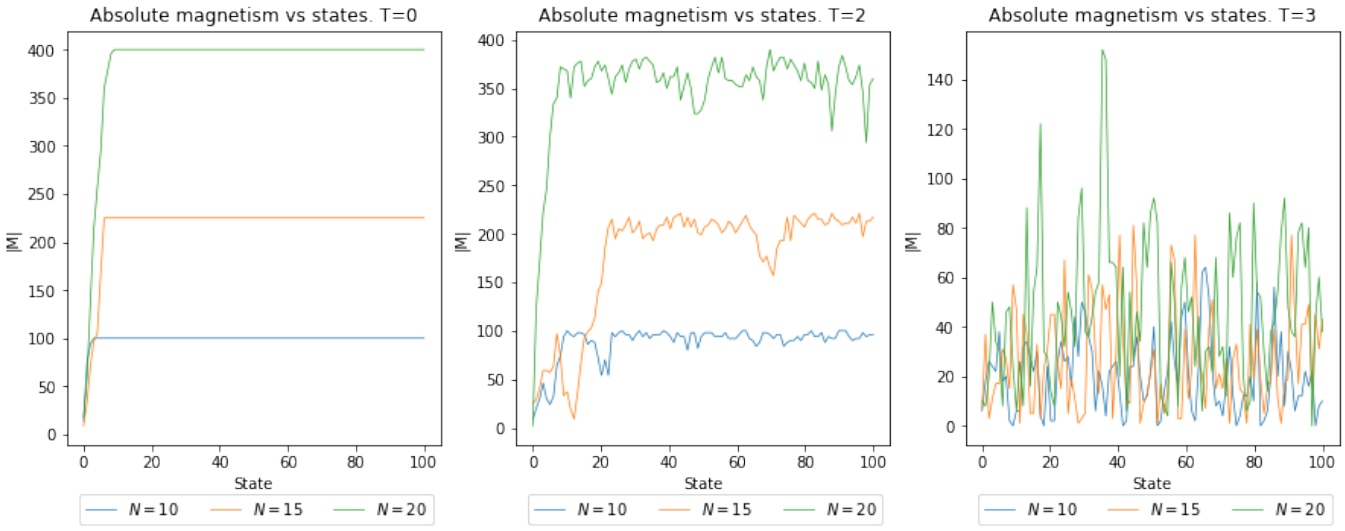

FIG. 13: Figure illustrating how near T_c the rate of convergence can vary.

[1] Feynman, Richard P.; Robert Leighton; Matthew Sands (1963). The Feynman Lectures on Physics, Vol. 2. Addison-Wesley. pp. Ch. 37.

[2] Velasco, S. Román, Francisco. (2007). Determining the Curie Temperature of Iron and Nickel. The Physics Teacher. 45. 387-389. 10.1119/1.2768702.

[3] Onsager, Lars (1944), "Crystal statistics. I. A two-dimensional model with an order-disorder transition", Physical Review, Series II, 65 (3–4): 117–149, Bibcode:1944PhRv...65..117O, doi:10.1103/PhysRev.65.117, MR 0010315

[4] Stephen L. Eltinge (2015), Numerical Ising Model Simulations on Exactly Solvable and Randomized Lattices, viewed 11/11/2019, $< http://web.mit.edu/8.334/www/grades/projects/projects15/EltingeStephen.pdf >$

[5] Ashcroft, Neil W.; Mermin, N. David (1976). Solid state phys. New York, Holt, Rinehart and Winston. p. 135. ISBN 978-0-03-083993-1.

[6] Richard Fitzpatrick (2006), The Ising Model, viewed 11/11/2019, $< http://farside.ph.utexas.edu/teaching/329/lectures/node110.html >$.